On the kernel and particle consistency in smoothed particle hydrodynamics

Leonardo Di G. Sigalotti[a,b,*], Jaime Klapp[c,d], Otto Rendón[b], Carlos A. Vargas[a], Franklin Peña-Polo[d,b]

[a]*Área de Física de Procesos Irreversibles, Departamento de Ciencias Básicas, Universidad Autónoma Metropolitana-Azcapotzalco (UAM-A), Av. San Pablo 180, 02200 México D.F., Mexico*
[b]*Centro de Física, Instituto Venezolano de Investigaciones Científicas (IVIC), Apartado Postal 20632, Caracas 1020-A, Venezuela*
[c]*Departamento de Física, Instituto Nacional de Investigaciones Nucleares (ININ), Carretera México-Toluca km. 36.5, La Marquesa, 52750 Ocoyoacac, Estado de México, Mexico*
[d]*ABACUS-Centro de Matemáticas Aplicadas y Cómputo de Alto Rendimiento, Departamento de Matemáticas, Centro de Investigacin y de Estudios Avanzados (Cinvestav-IPN), Carretera México-Toluca km. 38.5, La Marquesa, 52740 Ocoyoacac, Estado de México, Mexico*

Abstract

The problem of consistency of smoothed particle hydrodynamics (SPH) has demanded considerable attention in the past few years due to the ever increasing number of applications of the method in many areas of science and engineering. A loss of consistency leads to an inevitable loss of approximation accuracy. In this paper, we revisit the issue of SPH kernel and particle consistency and demonstrate that SPH has a limiting second-order convergence rate. Numerical experiments with suitably chosen test functions validate this conclusion. In particular, we find that when using the root mean square error as a model evaluation statistics, well-known corrective SPH schemes, which were thought to converge to second, or even higher order, are actually first-order accurate, or at best close to second order. We also find that observing

---

[*]Corresponding author
Email addresses: `leonardo.sigalotti@gmail.com` (Leonardo Di G. Sigalotti), `jaime.klapp@inin.gob.mx` (Jaime Klapp), `ottorendon@gmail.com` (Otto Rendón), `carlosvax@gmail.com` (Carlos A. Vargas), `franklin.pena@gmail.com` (Franklin Peña-Polo)

the joint limit when $N \to \infty$, $h \to 0$, and $n \to \infty$, as was recently proposed by Zhu et al., where N is the total number of particles, h is the smoothing length, and n is the number of neighbor particles, standard SPH restores full C^0 particle consistency for both the estimates of the function and its derivatives and becomes insensitive to particle disorder.

Keywords: Numerical methods (mathematics); Smoothed particle hydrodynamics (SPH); Consistency; Kernel consistency; Particle consistency

---

1. Introduction

The method of smoothed particle hydrodynamics (SPH) was introduced in the literature independently by Gingold and Monaghan [7] and Lucy [15] for modeling astrophysical flow problems. Since then the method has been widely applied to different areas of science and engineering due to its simplicity and ease of implementation. At the same time, the method has been improved over the years to overcome major shortcomings and deficiencies. One longstanding drawback of standard SPH is the particle inconsistency, which is an intrinsic manifestation of the lack of integrability of the kernel approximation in its spatially discretized form, resulting in a loss of accuracy. In practical applications, SPH inconsistency arises when the support domain of the kernel is truncated by a model boundary, for irregularly distributed particles even in the absence of kernel truncation, and for spatially adaptive calculations where a variable smoothing length is employed.

Several corrective strategies have been proposed to restore particle consistency in SPH calculations. A simple correction technique was first advanced by Li and Liu [11] and Liu at al. [14], where the kernel itself is modified to ensure that polynomial functions up to a given degree are exactly interpolated. A kernel gradient correction, allowing for the exact evaluation of the gradient of a linear function, was further proposed by Bonet and Lok [2] based on a variational formulation of SPH. A general approach to the construction of kernel functions that obey the consistency conditions of SPH in continuous form and describe the compact supportness requirement was presented by Liu et al. [13]. A drawback of this approach is that the reconstructed smoothing functions may be partially negative, non-symmetric, and non-monotonically decreasing, thereby compromising the stability of the numerical simulations.

2

More stable approaches for restoring consistency are based on Taylor series expansions of the kernel approximations of a function and its derivatives. In general, if up to m derivatives are retained in the series expansions, the resulting kernel and particle approximations will have $(m + 1)$th-order accuracy or mth-order consistency (i.e., C^m consistency). This approach was first developed by Chen et al. [5, 4] (their corrective smoothed particle method, or CSPM), which solves for the approximation of a function separately from that of its derivatives by neglecting all terms involving derivatives in the former expansion and retaining only first-order terms in the latter expansions. This scheme is equivalent to a Shepard's interpolation for the function [20], and so it should restore C^1 kernel and particle consistency for the interior regions and C^0 consistency at the boundaries. By retaining only first-order derivatives in the Taylor series expansions for the function and its derivatives and solving simultaneously the resulting set of linear equations (the FPM scheme), Liu and Liu [12] argued that C^1 kernel and particle consistency can be obtained for both interior and boundary regions. The FPM scheme was further improved by Zhang and Batra [26] (their MSPH scheme), where now up to second-order derivatives are retained in the Taylor series expansions. In principle, this method should restore C^2 consistency for the SPH approximation of the function (i.e., third-order convergence rates) and C^1 consistency for the first-order derivatives. However, when adding higher-order derivatives in the Taylor expansions, the number of algebraic linear equations to be solved increases rapidly, implying high computational costs. In addition, since the solution involves a matrix inversion, for some types of problems the stability of the scheme can be compromised by the conditioning of the matrix. A modified FPM approach, which is free of kernel gradients and leads to a symmetric corrective matrix was recently proposed by Huang et al. [10]. An alternative formulation based on the inclusion of boundary integrals in the kernel approximation of the spatial derivatives was reported by Macià et al. [16], which restores C^0 consistency at the model boundaries. A new SPH formulation, based on a novel piecewise high-order Moving-Least-Squares WENO reconstruction and on the use of Riemann solvers, that improves the accuracy of SPH in the presence of sharp discontinuities was recently reported by Avesani et al. [1].

A new strategy to ensure formal convergence and particle consistency with standard SPH has recently been devised by Zhu et al. [28] in the astrophysical context. In this approach, no corrections are required and full consistency is recovered provided that $N \to \infty$, $h \to 0$, and $n \to \infty$, where

N is the total number of particles, h is the smoothing length, and n is the number of neighbor particles within the kernel support. They found that if n is fixed, as is customary in SPH, consistency will not be guaranteed even though $N \to \infty$ and $h \to 0$ since there is a residual error that will not vanish unless n is allowed to increase with N as $n \sim N^{1/2}$. However, the systematic increase of n with improved resolution demands changing the interpolation kernel to a Wendland-type function [25], which, unlike traditional kernels, is free from the pairing instability when used to perform smoothing in SPH with large numbers of neighbors [6].

In this paper, we revisit the issue of kernel and particle consistency in SPH. We first demonstrate that the normalization condition of the kernel is independent of h, suggesting that its discrete representation depends only on n, consistently with the error analyses of Vaughan et al. [23] and Read et al. [21]. Although C^0 and C^1 kernel and particle consistency can be achieved by some corrective SPH methods, a simple observation shows that C^2 kernel consistency is difficult to achieve, implying an upper limit to the convergence rate of SPH in practical applications. Numerical experiments with suitably chosen test functions in two-space dimensions validate this conclusion. The paper is organized as follows. In Section 2, we discuss the issue of C^0 consistency and show that the normalization condition of the kernel is independent of h. The issue of higher-order consistency is considered in Section 3, where we show that C^2 consistency is affected by an inherent intrinsic diffusion, which arises as a consequence of the dispersion of the SPH particle positions relative to the mean. Section 4 outlines the importance of restoring C^1 consistency for the gradient. Finally, Section 5 presents numerical tests that demonstrate the convergence rates of the particle approximations and Section 6 contains the conclusions.

2. Normalization condition and C^0 consistency

As it is well-known, the starting point of SPH lies on the exact identity

$$f(\mathbf{x}) = \int_{\mathcal{R}^3} f(\mathbf{x}')\delta(\mathbf{x} - \mathbf{x}')d\mathbf{x}', \tag{1}$$

where $f = f(\mathbf{x})$ is some sufficiently smooth function, $\delta(\mathbf{x} - \mathbf{x}')$ is the Dirac-δ distribution, and the integration is taken over all space. The kernel approximation is obtained by replacing the Dirac-δ distribution by some kernel

interpolation function W such that

$$\langle f(\mathbf{x}) \rangle = \int_{\mathcal{R}^3} f(\mathbf{x}')W(|\mathbf{x} - \mathbf{x}'|, h)d\mathbf{x}', \qquad (2)$$

where $\langle f(\mathbf{x}) \rangle$ is the smoothed estimate of $f(\mathbf{x})$ and W must satisfy the following properties: (a) in the limit $h \to 0$ it becomes the Dirac-δ function so that $\langle f(\mathbf{x}) \rangle \to f(\mathbf{x})$, (b) it must satisfy the normalization condition

$$\int_{\mathcal{R}^3} W(|\mathbf{x} - \mathbf{x}'|, h)d\mathbf{x}' = 1, \qquad (3)$$

and (c) it must be positive definite, symmetric, and monotonically decreasing. Almost all modern applications of SPH assume that W has compact support, that is, $W(|\mathbf{x} - \mathbf{x}'|, h) = 0$ for $|\mathbf{x} - \mathbf{x}'| \geq kh$, where k is some integer that depends on the kernel function.

We shall first demonstrate that the normalization condition for a kernel satisfying the above properties is independent of the smoothing length h. This feature is tacitly assumed in the SPH literature. However, as we shall see later, it has important conceptual implications for the kernel consistency relations. For simplicity in exposition, let us restrict to one-space dimension and assume the kernel to be a Gaussian function such that

$$\delta(x - x') = \lim_{h \to 0} \frac{1}{\sqrt{2\pi}h} \exp\left[\frac{-(x - x')^2}{2h^2}\right]. \qquad (4)$$

Making the change $|x - x'| \to h|x - x'|$ in the Gaussian kernel, it is then easy to show the following scaling relation

$$W(h|x - x'|, h) = \frac{1}{h}W(|x - x'|, 1), \qquad (5)$$

which is indeed satisfied by all known SPH kernel functions. Similar forms follow in two- and three-space dimensions with $1/h$ replaced by $1/h^2$ and $1/h^3$, respectively. Now expanding in Taylor series $f(x')$ around $x' = x$ with $x \to hx$ and $x' \to hx'$, we obtain

$$f(hx') = \sum_{l=0}^{\infty} \frac{1}{l!}h^l f^{(l)}(hx)(x' - x)^l, \qquad (6)$$

which when inserted in the kernel approximation (2) yields

$$\langle f(hx) \rangle = \sum_{l=0}^{\infty} \frac{1}{l!}h^l f^{(l)}(hx) \int_{\mathcal{R}} (x' - x)^l W(|x - x'|, 1)dx', \qquad (7)$$

5

where we have made $dx' \to hdx'$ in the integrand and used the scaling relation (5). Using the Gaussian kernel, the integral in Eq. (7) when $l = 0$ is just the probability function and is exactly one, yielding the condition

$$\int_{\mathcal{R}} W(|x - x'|, 1)dx' = 1. \tag{8}$$

Therefore, the normalization condition is independent of h provided that the kernel interpolation obeys the scaling relation (5). Alternatively, in the SPH literature the kernels are usually defined in terms of the dimensionless parameter $q = |x - x'|/h$ such that $W(|x - x'|, h) = W(q)/h$, which is not the same as Eq. (5) because q depends explicitly on h. In addition, all terms in Eq. (7) with l odd vanish because of the symmetry of the kernel function, while only those with l even survive. Therefore, using Eq. (8) and retaining only the $l = 2$ term in Eq. (7), we obtain

$$\langle f(hx) \rangle = f(hx) + \frac{1}{2}h^2 f''(hx) \int_{\mathcal{R}} (x' - x)^2 W(|x - x'|, 1)dx' + O(h^4), \tag{9}$$

which expresses that the kernel approximation of a function is second-order accurate and therefore has C^1 consistency for an unbounded domain. Thus, for such infinitely extended domains C^1 consistency requires that C^0 consistency be satisfied according to Eq. (8). As was pointed out by Liu and Liu [12] and formally demonstrated by Vaughan [22], for a bounded domain the kernel approximation (2) needs be replaced by the integral form of the Shepard interpolant to guarantee C^0 consistency near a model boundary. Equation (9) bears some resemblance with the expression of the error derived by Vaughan et al. [23], where the contribution to the error due to the smoothing length can be separated from that due to the discretized form of the integral, which, being independent of h, will directly depend on the number of neighbors within the kernel support.

The SPH discretization makes reference to a set of Lagrangian particles which may, in general, be disordered. If we consider a finite model domain $\Omega \in \mathcal{R}$ and divide it into N sub-domains, labeled Ω_a, each of which contains a Lagrangian particle a at position $x_a \in \Omega_a$, the discrete form of Eq. (8) becomes

$$\sum_{b=1}^{N} W_{ab} \Delta x_b = O(1), \tag{10}$$

where $W_{ab} = W(|x_a - x_b|, 1)$. In general, the above summation is not exactly one. In this approximation, the error depends on the number of particles N

and how these are actually distributed. If the kernel has compact support, then the above summation is over the number of particles n within a length over which the kernel itself does not vanish, i.e., $|x_a - x_b| < kh$. In this case, the error scales as $\sim n^{-\alpha}$, where $\alpha = 0.5$ for a truly random distribution of particles and $\alpha = 1$ for quasi-ordered patterns [28]. In either case, if n is sufficiently large the discrete normalization condition becomes sufficiently close to one ensuring C^0 particle consistency. This will certainly require to scale n with N as $\sim N^{0.5}$ as the resolution is improved [28].

The discrete form (10) losses C^0 consistency for irregularly distributed particles even far away from the model boundaries because node disorder results in a noise error, which scales with n as $\sim n^{-1} \ln n$ [17]. C^0 particle consistency is equivalent to demand that the homogeneity of space is not affected by the process of spatial discretization, which in turn has, as a consequence, the conservation of linear momentum [24]. In other words, the SPH interpolation has to be independent of a rigid-body translation of the coordinates. To see this, consider the discrete form of Eq. (2) for the position vector $\mathbf{x} = (x, y, z)$, i.e.,

$$\langle \mathbf{x} \rangle_a = \sum_{b=1}^{n} \mathbf{x}_b W_{ab} \Delta V_b, \tag{11}$$

where $W_{ab} = W(|\mathbf{x}_a - \mathbf{x}_b|, 1)$ and ΔV_b is the volume of the sub-domain Ω_b within which particle b lies. In SPH simulations, it is common practice to evaluate ΔV_b as the ratio m_b / ρ_b, where m_b and ρ_b refer to the mass and density of particle b, respectively. According to Eq. (11), the estimate of the transformed coordinates $\mathbf{x}' = \mathbf{x} + \Delta \mathbf{x}$ is

$$\langle \mathbf{x}' \rangle_a = \sum_{b=1}^{n'} \mathbf{x}'_b W'_{ab} \Delta V'_b, \tag{12}$$

where $W'_{ab} = W(|\mathbf{x}'_a - \mathbf{x}'_b|, 1)$. Preservation of space homogeneity under uniform translation demands that $\langle \Delta \mathbf{x} \rangle = \Delta \mathbf{x}$ so that $\langle \mathbf{x}' \rangle_a = \langle \mathbf{x} \rangle_a + \Delta \mathbf{x}$. Replacing $\mathbf{x}'_b$ by $\mathbf{x}_b + \Delta \mathbf{x}$ in Eq. (12) yields

$$\langle \mathbf{x}' \rangle_a = \langle \mathbf{x} \rangle_a + \Delta \mathbf{x} \sum_{b=1}^{n} W_{ab} \Delta V_b, \tag{13}$$

where we have made $W'_{ab} \Delta V'_b = W_{ab} \Delta V_b$ and $n' = n$ because under solid-body translation the coordinates of a point are independent of the translation of

7

the coordinates axes. Therefore, Eq. (13) expresses that homogeneity of the discretized space is recovered by the SPH interpolation only if the condition

$$\sum_{b=1}^{n} W_{ab}\Delta V_b = 1, \tag{14}$$

is satisfied exactly. A simple way to enforce this condition at a model boundary is to use a discrete Shepard interpolation [20, 2, 22], where the kernel function is normalized according to

$$W_{ab} \rightarrow \frac{W_{ab}}{\sum_{b=1}^{n} W_{ab}\Delta V_b}, \tag{15}$$

or alternatively, to use huge numbers of particles such that the limits $N \rightarrow \infty$, $h \rightarrow 0$, and $n \rightarrow \infty$ are achieved in an approximate sense [28].

3. Higher-order consistency

For the sake of simplicity we shall restrict ourselves again to one-space dimension. However, the analysis of this and the preceding section can be easily generalized to higher dimensions. If a polynomial of degree m is exactly reproduced by an approximation, then we say that it has C^m consistency and the following family of integral conditions must hold for the kernel

$$\int_{\mathcal{R}} (x - x')^l W(|x - x'|, h)dx' = \delta_{l0}, \tag{16}$$

for $l = 0,1,2,...m$, where $\delta_{l0}(= 1$ for $l = 0$ and $= 0$ for $l \neq 0)$ is the Kronecker delta. Using the scaling relation (5) and making $|x - x'| \rightarrow h|x - x'|$, the integrals in Eq. (16) can be rewritten as

$$\int_{\mathcal{R}} (x - x')^l W(|x - x'|, 1)dx' = h^{-l}\delta_{l0}. \tag{17}$$

For $l = 0$, Eq. (17) states the normalization condition (8), while for $l = 1$ it states the symmetry property of the kernel. Using the Gaussian kernel, we may show that this integral is exactly zero for an infinitely extended domain, implying C^1 kernel consistency. Thus, if C^1 consistency is achieved, then C^0 consistency is automatically guaranteed.

For $l = 2$, Eq. (17) reduces to

$$\int_{\mathcal{R}} (x - x')^2 W(|x - x'|, 1)dx' = 0, \tag{18}$$

8

which must be satisfied in order to ensure C^2 consistency for the kernel approximation. We note that this integral already appears in Eq. (9) as a finite source of error and it does not vanish unless the kernel approaches the Dirac-δ function. Using Eqs. (2) and (8), we may evaluate this integral to obtain

$$
\begin{aligned}
\int_{\mathcal{R}} (x - x')^2 W(|x - x'|, 1) dx' &= x^2 - 2x\langle x \rangle + \langle x^2 \rangle \\
&= (x - \langle x \rangle)^2 + \left(\langle x^2 \rangle - \langle x \rangle^2 \right). \quad (19)
\end{aligned}
$$

If C^1 consistency is guaranteed by the kernel approximation then $x = \langle x \rangle$, and the above integral becomes

$$
\int_{\mathcal{R}} (x - x')^2 W(|x - x'|, 1) dx' = \langle x^2 \rangle - \langle x \rangle^2 \neq 0, \quad (20)
$$

which implies that C^2 kernel consistency is not achieved even though C^0 and C^1 consistencies are satisfied, unless $W(|x - x'|, 1) \to \delta(x - x')$, or equivalently, $N \to \infty$, $h \to 0$, and $n \to \infty$ as suggested by Zhu et al. [28], in which case $\langle x^2 \rangle = \langle x \rangle^2$. It is evident from Eq. (20) that the lack of C^2 consistency is due to an intrinsic diffusion $\sigma^2 = \langle x^2 \rangle - \langle x \rangle^2$, which is equal to the variance of x. This is a measurement of the dispersion (or spread) of the particle positions relative to the mean. This also explains why SPH becomes inherently unstable when estimating second-order derivatives. For instance, it is well-known that SPH formulations based on the second-order derivatives of the kernel are highly sensitive to particle disorder, where dispersion may be enhanced by the presence of non-uniform velocity fields [8]. This observation certainly implies that in practical applications SPH has a limiting second-order convergence.

4. SPH approximation of first-order derivatives

The kernel approximation of the gradient of a function can be obtained from Eq. (2) by replacing f by ∇f and integrating by parts [17], to yield

$$
\langle \nabla f(\mathbf{x}) \rangle = \int_{\mathcal{R}^3} f(\mathbf{x}') \nabla W(|\mathbf{x} - \mathbf{x}'|, h) d\mathbf{x}', \quad (21)
$$

which can be approximated to mth-order accuracy if the following conditions are satisfied [13]

$$
\int_{\mathcal{R}^3} (\mathbf{x} - \mathbf{x}')^l \nabla W(|\mathbf{x} - \mathbf{x}'|, 1) d\mathbf{x}' = \mathbf{I}_{l1}, \quad (22)
$$

9

where $l = 0,1,2,...m$ and $\mathbf{I}_{l1}$ is a tensor of rank m whose components are all equal to δ_{l1}. For $l = 0$, Eq. (22) is equivalent to the condition that the kernel function must vanish at the surface of integration, while for $l = 1$ it reduces to

$$\int_{\mathcal{R}^3} (\mathbf{x} - \mathbf{x}')\nabla W(|\mathbf{x} - \mathbf{x}'|, h)d\mathbf{x}' = \mathbf{I}, \tag{23}$$

where $\mathbf{I}$ is the identity matrix. Satisfaction of this condition means that the isotropy of space is not affected by the SPH kernel approximation [24] and, as a consequence, angular momentum is preserved [2]. The same statement holds for the particle approximation. In other words, the interpolation must be independent of a rotation of the coordinate axes. In order to see this, let us consider for simplicity only small rotations so that the coordinates change according to the transformation

$$
\begin{aligned}
\mathbf{x}' &= \mathbf{x} - d\mathbf{w} \times \mathbf{x} \\
&= \mathbf{x} - \mathbf{x} \cdot \nabla(d\mathbf{w} \times \mathbf{x}),
\end{aligned}
\tag{24}
$$

where $d\mathbf{w}$ is the differential rotation vector. Under solid-body rotation, the coordinates of a point are independent of the rotation of the coordinate axes and therefore

$$\langle \nabla(d\mathbf{w} \times \mathbf{x})\rangle_a = \nabla(d\mathbf{w} \times \mathbf{x}), \tag{25}$$

or alternatively, using the discretized form of Eq. (21)

$$
\begin{aligned}
\langle \nabla(d\mathbf{w} \times \mathbf{x})\rangle_a &= \sum_{b=1}^{n} (d\mathbf{w} \times \mathbf{x})_b \nabla_a W_{ab} \Delta V_b \\
&= \sum_{b=1}^{n} [\mathbf{x} \cdot \nabla(d\mathbf{w} \times \mathbf{x})]_b \nabla_a W_{ab} \Delta V_b \\
&= \nabla(d\mathbf{w} \times \mathbf{x}) \cdot \sum_{b=1}^{n} \mathbf{x}_b \nabla_a W_{ab} \Delta V_b,
\end{aligned}
\tag{26}
$$

which implies that the condition

$$\sum_{b=1}^{n} \mathbf{x}_b \nabla_a W_{ab} \Delta V_b = \mathbf{I}, \tag{27}$$

must be satisfied exactly in order to preserve the isotropy of the discretized space and ensure angular momentum conservation.

10

5. Numerical analysis

In this section, we describe the results of a series of numerical experiments in two-space dimensions for two different test functions, namely,

$$f_1(x, y) = \sin \pi x \sin \pi y, \tag{28}$$

and

$$f_2(x, y) = x^{5/2} \left(20y^5 + 8xy^3 + x^2y^2 + 1 \right), \tag{29}$$

over the intervals $x \in [0, 1]$ and $y \in [0, 1]$, in order to check their reproducibility for both regularly and irregularly distributed particles. We analyze the convergence rate of the SPH approximations for the functions and their derivatives using five different methods: (a) the standard SPH, (b) the CSPM method of Chen et al. [5, 4], (c) the FPM scheme of Liu and Liu [12], (d) the MSPH method of Zhang and Batra [26], and (e) the methodology recently proposed by Zhu et al. [28], which we label SPHn to distinguish it from the standard SPH. Similarly, when CSPM and FPM are run with the Wendland function and varying number of neighbors we shall label them CSPMn and FPMn, respectively. Unlike the other SPH methods, MSPH includes second-order derivatives in the Taylor series expansions and therefore it should restore C^2 kernel and particle consistency, implying that it should converge faster than second-order accuracy in contrast to the statement of Eq. (20), which predicts a second-order limit to the convergence rate of SPH. The cubic B-spline kernel [19] with a fixed number of neighbors ($n \approx 13$) is used for standard SPH, CSPM, FPM, and MSPH, i.e.,

$$W(q, h) = \frac{15}{7\pi h^2} \begin{cases} \frac{2}{3} - q^2 + \frac{1}{2}q^3 & \text{if } 0 \leq q < 1, \\ \frac{1}{6}(2 - q)^3 & \text{if } 1 \leq q < 2, \\ 0 & \text{if } q \geq 2, \end{cases} \tag{30}$$

where $q = |\mathbf{x} - \mathbf{x}'|/h$, while a Wendland C^4 function [25, 6]

$$W(q, h) = \frac{9}{\pi h^2} \begin{cases} (1 - q)^6 \left(1 + 6q + \frac{35}{3}q^2 \right) & \text{if } q < 1, \\ 0 & \text{if } q \geq 1, \end{cases} \tag{31}$$

is employed for standard SPH, CSPM, and FPM with varying number of neighbors as the resolution is increased (i.e., schemes SPHn, CSPMn, and FPMn). In these analyses no boundary treatments are implemented at the borders of the particle configurations.

We vary the spatial resolution from 625 to 562500 particles for both distributions (see first column of Table 1) and measure the convergence rates of the function estimates in terms of the root mean square error (RMSE)

$$\text{RMSE}(f) = \sqrt{\frac{1}{N} \sum_{a=1}^{N} (f_a^{\text{exact}} - f_a^{\text{num}})^2}, \tag{32}$$

which is closely related to the L_2-norm. Identical forms to Eq. (32) are also used to assess the errors in the estimates of the derivatives. Since the SPH errors are expected to have a normal rather than a uniform distribution, the RMSE will provide a better representation of the error distribution than other statistical metrics [3]. Compared to the mean absolute error (MAE), which is more closely related to the L_1-norm, the RMSE gives a higher weighting toward large errors in the sample than the mean average error and therefore it is superior at revealing model performance differences. In fact, when both metrics are calculated, the RMSE is always larger than the MAE.

Table 1: Spatial resolution parameters for the calculations

Number of SPH particles N	Number of neighbors n	Smoothing length h
625	213	0.342
2500	556	0.271
5625	973	0.237
10000	1436	0.215
15625	1933	0.200
22500	2472	0.188
30625	3041	0.179
40000	3648	0.170
62500	4880	0.158
90000	6288	0.149
160000	9216	0.136
250000	12416	0.126
562500	21328	0.110

In the calculations with schemes SPHn, CSPMn, and FPMn, where the Wendland C^4 kernel is used and the number of neighbors (n) is varied with N, the quality of the SPH estimates is analyzed by examining the standard

deviation of the SPH evaluated functions and derivatives as a function of n. This provides a measure of the rate at which the inconsistency of the SPH estimates declines as the number of neighbors increases, consistently with the expected dependence of the SPH particle discretization error on n [17]. For these tests, we use the parameterizations provided by Zhu et al. [28] and allow h to vary with N as $h = N^{-1/6}$. With this choice we obtain the scaling relations $n \approx 2.81N^{0.675}$ and $h \approx 1.29n^{-0.247}$ for n and h, respectively. Figure 1 shows the variation of h with n. Based on a balance between the SPH smoothing and discretization errors, Zhu et al. [28] derived the parameterizations $h \propto N^{-1/\beta}$ and $n \propto N^{1-3/\beta}$ for $\beta \in [5, 7]$. An intermediate value of $\beta \sim 6$ is appropriate when the smoothing is performed with the Wendland kernel (31) on a quasi-ordered particle configuration. Thus, choosing the proportionality factor of the scaling $h \propto N^{-1/6}$ as exactly unity gives exponents for the dependences of n on N and of h on n that are slightly larger than 0.5 and $-1/3$, respectively, as suggested by the parameterizations of Zhu et al. [28]. However, preliminary tests with exponents close to the suggested values produced a similar variation of h with n as shown in Fig. 1, while the convergence rates for SPHn, CSPMn, and FPMn remained essentially the same (see next Section). We see that for small values of n the smoothing length decreases rapidly as the number of neighbors increases and then more slowly at large n, asymptotically approaching zero as $n \to \infty$ as needed to restore particle consistency. The second and third columns of Table 1 list the number of neighbors and values of the smoothing length, respectively, as they were obtained from the above scalings.

5.1. Regularly distributed particles

As we have discussed before, C^m consistency defines the property of a numerical scheme to reproduce a given field function or distribution to $(m + 1)$th-order accuracy. Therefore, in order to assess the consistency of the several methods we first start by analyzing their convergence rates on the test functions f_1 and f_2 and their derivatives for a perfectly regular distribution of particles. Table 2 lists the calculated convergence rates as obtained from the different SPH methods. For all methods, the convergence rate corresponds to the slope resulting from a least squares fitting of the RMSE data points.

The dependence of the RMSE of the SPH function estimates on the effective number of particles N is shown in Fig. 2 for f_1 (left) and f_2 (right). We see that standard SPH exhibits very poor convergence rates. For the estimate of f_1, the solution converges to $N^{-0.75}$ for the first four resolutions, while at

Table 2: Convergence rates of RMSE metrics for a regular distribution of SPH particles

Type of function	SPH	CSPM	FPM	MSPH	SPHn	CSPMn	FPMn
f_1	0	-0.76	-1.0	-1.76	-0.97	-0.92	-1.0
$f_{1,x}$	+0.51	-0.77	-0.77	-1.0	-0.77	-0.94	-0.95
$f_{1,y}$	+0.51	-0.77	-0.77	-1.0	-0.77	-0.94	-0.95
$f_{1,xx}$	——	——	——	-0.75	——	——	——
$f_{1,xy}$	——	——	——	-1.0	——	——	——
$f_{1,yy}$	——	——	——	-0.75	——	——	——
f_2	-0.28	-0.76	-1.0	-1.76	-0.78	-0.92	-0.98
$f_{2,x}$	-0.26	-0.75	-0.76	-1.0	-0.77	-0.91	-0.93
$f_{2,y}$	-0.26	-0.75	-0.77	-1.0	-0.77	-0.91	-0.93
$f_{2,xx}$	——	——	——	-0.62	——	——	——
$f_{2,xy}$	——	——	——	0	——	——	——
$f_{2,yy}$	——	——	——	-0.01	——	——	——

higher resolutions the RMSE reaches a plateau. Thus, in terms of the absolute error, the highest resolution fails to give the best results with standard SPH. Conversely, for the estimates of f_2 the solution converges to $N^{-0.28}$ for all values of N. Faster convergence rates, i.e., $N^{-0.76}$, N^{-1}, and $N^{-1.76}$ are obtained for CSPM, FPM, and MSPH, respectively, for both the estimates of f_1 and f_2. As expected, the fastest convergence is achieved by the MSPH scheme, which is effectively close to second-order accuracy. Therefore, MSPH is at best C^1-consistent, while FPM exhibits C^0 consistency. When passing from FPM to CSPM the accuracy of SPH degrades from N^{-1} to $N^{-0.76}$, implying that CSPM is not even restoring full C^0 consistency. These results validate the arguments presented in Section 3, which show that SPH has a limiting convergence rate of N^{-2}.

In passing, we note that Zhang and Batra [27] reported convergence rates for their MSPH scheme of $N^{-3.52}$ when analyzing a sinusoidal test function. Although they claim to have used an RMSE, we find that using the square of the RMSE, i.e., the mean squared error (MSE), which corresponds effectively to an L_2-norm error, the convergence rate of MSPH improves to $N^{-3.52}$, which surprisingly coincides with the rate reported by them. This clearly suggests that the convergence rate found by Zhang and Batra [27] are more likely based on an MSE than on an RMSE, and therefore it does not represent a correct estimate of the actual errors. It is often encountered in the SPH literature that the MAE, or L_1-norm error, is also used to determine conver-

gence rates. However, since the SPH errors are not uniformly distributed, the MAE is likely to remove information because it gives the same weight to all errors. In contrast, the RMSE consists of squaring the magnitude of the errors before they are averaged, and so it gives a relatively higher weight to errors with larger absolute values [3]. In this sense, the RMSE represents a better statistical metric than the MAE because it provides not only a good indicator of the average performance model but also a better representation of the error distribution.

When standard SPH is run with the Wendland kernel and varied number of neighbors according to the scaling relation $n \approx 2.81N^{0.675}$, the convergence rate effectively improves from a near plateau to $N^{-0.97}$ for the estimate of f_1 and from $N^{-0.28}$ to $N^{-0.78}$ for the estimate of f_2. These rates are comparable to those of CSPM and FPM with a fixed number (~ 13) of neighbors. Evidently, increasing the number of neighbors while decreasing the smoothing length with increasing resolution has the benefit of reducing the SPH discretization errors, thereby allowing standard SPH to restore C^0 consistency. However, working with varying number of neighbors as N is increased has only a moderate effect on CSPM, whose convergence rate improves from $N^{-0.76}$ to $N^{-0.92}$, and essentially no effect on FPM, which maintains the same convergence rate as with fixed n. Figure 3 shows the standard deviation of the estimates of f_1 and f_2 as a function of n as obtained with SPHn, CSPMn, and FPMn. For all three methods, the standard deviation decreases as we increase the number of neighbors in the SPH estimates. We observe an approximate n^{-1} trend for all cases, which is appropriate for a quasi-regular distribution of particles [28]. This closely follows the expected dependence of the SPH discretization error on the number of neighbors for a quasi-ordered pattern [17], $\epsilon \propto \log(n)/n$, which was then further parameterized by Zhu et al. [28] as $\epsilon \propto n^{-1}$. As n is further increased and h is reduced as shown in Fig. 1, the normalization condition in discrete form approaches unity. In this limit, the kernel approaches the Dirac-δ distribution and the homogeneity of the discretized space is fully recovered, implying that the field function is exactly reproduced.

The convergence rates of the first-order derivatives $(f_{1,x}, f_{1,y})$ and $(f_{2,x}, f_{2,y})$ are depicted in Figs. 4 and 5, respectively. The convergence rate of standard SPH has a positive slope for the estimates of both the x- and y-derivatives of f_1, implying that the numerical results diverge from the actual values at all resolutions. This is a consequence of the RMSE plateauing for the estimate of f_1 (see Fig. 2). In contrast, the RMSE of the derivative estimates of f_2

15

are seen to scale as $N^{-0.26}$ for both derivatives (see Table 2), while for CSPM the estimates of the derivatives converge to almost the same rates as the estimate of the function itself, i.e., as $N^{-0.77}$ for the smoothed derivatives of f_1 and $N^{-0.75}$ for those of f_2. As expected, the convergence rate of the derivatives degrades to less than first-order for the FPM scheme for both test functions and to first-order for the MSPH scheme, implying C^0 particle consistency for the first-order derivatives with this latter method. Almost C^0 consistency is also restored for the estimates of the second-order derivatives of f_1. The estimates of $f_{1,xx}$ and $f_{2,xx}$ share the same convergence rate, i.e., $N^{-0.75}$, while the RMSE of $f_{1,xy}$ scales as N^{-1}. This is not surprising because $f_{1,xx} = f_{1,yy} = -\pi^2 f_1$, while $f_{1,xy} = \pi^2 \cos \pi x \cos \pi y$. However, for the polynomial function f_2, C^0 consistency is lost as the RMSE of the estimates of $f_{2,xy}$ and $f_{2,yy}$ follows a plateau for all resolution runs, while an $N^{-0.62}$ rate is observed for $f_{2,xx}$ (see Table 2). The results show that SPHn, CSPMn, and FPMn all exhibit approximately first-order convergence rates for both the function and its derivatives. This is one advantage of running with varying number of neighbors over maintaining n fixed with increasing overall resolution, which restores the same order of consistency for both the particle estimates of the function and its derivatives.

5.2. Irregularly distributed particles

It is well-known that in true SPH simulations, pressure forces mediate between SPH particles, which tend to regulate the distribution of neighbors into quasi-regular patterns. In some instances, the particle distribution can become highly irregular as in the case of highly turbulent flows. In either case it is unlikely that particles will be accommodated in a truly random distribution because the continuity property of the flow will prevent particles from moving randomly even under highly non-uniform velocity fields [17, 18]. However, when particles are arranged in an irregular pattern, a loss of consistency may arise as a consequence of noise on small scales, resulting in an error which scales as $\sim n^{-1} \ln n$ [17]. Moreover, if the degree of particle disorder increases, the performance of SPH decreases [9]. Therefore, it is of interest to explore the behavior of the different SPH methods on particle disorder by maintaining exactly the same parameters as in the previous section.

Figure 6 depicts the irregular placement of particles for the lowest resolution case (625 particles) on a $[0, 1] \times [0, 1]$ square. The same degree of disorder was maintained for all resolutions shown in Table 1. The results of the calculations are condensed in Table 3, where the convergence rates of the

test functions and their derivatives are shown. Figure 7 displays the dependence of the RMSE for the estimates of f_1 (left) and f_2 (right) on resolution. Comparing the results in Table 3 with those in Table 2 we see that in general the convergence rates of CSPM, FPM, and MSPH slow down for an irregular pattern. However, schemes SPHn, CSPMn, and FPMn with varying number of neighbors are much less sensitive to particle disorder and exhibit almost the same convergence rates independently of whether the particle distribution is regular or irregular. The standard deviation of the function estimates against the number of neighbors is displayed in Fig. 8. A trend close to n^{-1} is again reproduced for all three methods. Hence, the small-scale noise induced by particle disorder does not seem to affect the rate of decay of the standard deviation of the function estimates with n. In fact, the standard deviations show very small discrepancies from an exact partition of unity for both the regular and irregular point sets. For truly random points, Zhu et al. [28] found that the error distribution will follow an $n^{-0.5}$ trend. However, in actual SPH flow simulations the randomness in the particle distribution is expected to be closer to an irregular (or quasi-random) sequence, where the spatial particle density is approximately uniform, rather than to a random one, where large contrasts may exist in particle density. Therefore, realistic applications may well fall midway between n^{-1} and $n^{-0.5}$ [28, 9]. However, our results indicate that the dependence of the standard deviation on n could be more biased toward n^{-1} for irregular particle configurations.

Table 3: Convergence rates of RMSE metrics for an irregular distribution of SPH particles

Type of function	SPH	CSPM	FPM	MSPH	SPHn	CSPMn	FPMn
f_1	-0.07	-0.59	-0.99	-1.53	-1.02	-0.92	-1.0
$f_{1,x}$	+0.52	-0.62	-0.62	-1.10	-0.78	-0.94	-0.94
$f_{1,y}$	+0.51	-0.62	-0.62	-1.13	-0.78	-0.94	-0.94
$f_{1,xx}$	——	——	——	-0.59	——	——	——
$f_{1,xy}$	——	——	——	-0.65	——	——	——
$f_{1,yy}$	——	——	——	-0.72	——	——	——
f_2	-0.18	-0.59	-0.99	-1.53	-0.77	-0.93	-1.0
$f_{2,x}$	-0.13	-0.67	-0.76	-1.08	-0.78	-0.93	-0.94
$f_{2,y}$	-0.12	-0.65	-0.64	-1.11	-0.78	-0.92	-0.94
$f_{2,xx}$	——	——	——	-0.73	——	——	——
$f_{2,xy}$	——	——	——	-0.02	——	——	——
$f_{2,yy}$	——	——	——	-0.03	——	——	——

17

For completeness, Figs. 9 and 10 depict the convergence rates of the smoothed derivatives of f_1 and f_2, respectively. The trends are similar to those displayed in Figs. 4 and 5 for a regular distribution of particles, except for the runs with MSPH for which the variations of the RMSE with N shows up and down turns, which are considerably more pronounced for the estimates of f_1 than for those of f_2. This zigzag behavior is indicative of MSPH being more sensitive to particle disorder when estimating derivatives. Similar erratic behaviors are also observed for the RMSE of the estimates of the second-order derivatives, except for the solutions of $f_{2,xy}$ and $f_{2,yy}$, which fail to converge because their RMSE follows a plateau for all resolution runs. As noted earlier, the convergence rates of the smoothed estimates of the second-order derivatives given in Tables 2 and 3 correspond to least squares fittings of the numerical errors.

In general, the convergence rates of the estimates of the first- and second-order derivatives slow down when the smoothing is performed on an irregular distribution of points. This is the case of standard SPH, CSPM, FPM, and MSPH with a fixed number of neighbors. However, if we compare the last three columns of Tables 2 and 3, we see that there are little differences between the convergence rates of SPHn, CSPMn, and FPMn for regular and irregular particle distributions. As n is increased with resolution, the discretization error, which scales as n^{-1}, decreases, making the calculations with varied number of neighbors much less sensitive to particle disorder. Similarly to the regular configuration, the convergence rate of standard SPH for the estimates of f_1 improves from $N^{-0.07}$ to first-order accuracy ($N^{-1.02}$), while for f_2 the speed of convergence increases from $N^{-0.18}$ to $N^{-0.77}$, implying that C^0 consistency of standard SPH is restored when working with varied number of neighbors. First-order convergence rates are also observed with SPHn for the estimates of the first-order derivatives. Full C^0 consistency is also restored with CSPMn for both the estimates of f_1 and f_2 and their first derivatives. Thus, the same order of consistency is maintained for the approximation of the function and its derivatives even for a disordered point set. This is also seen when comparing FPM with FPMn, where the accuracy of the approximation for the derivatives becomes close to first order for both test functions for the latter scheme. Hence, as long as $N \to \infty$, $h \to 0$, and $n \to \infty$ we expect that the SPH estimates of the derivatives converge essentially at the same rate as the estimate of the function. In this limit, the approximation becomes insensitive to particle disorder.

18

6. Conclusions

In this paper, we have re-examined the problem of kernel and particle consistency in the smoothed particle hydrodynamics (SPH) method. In particular, we first demonstrate with a simple observation that any kernel function that is suitable for SPH interpolation can be scaled with respect to the smoothing length in such a way that the kernel normalization condition as well as the family of consistency relations become independent of the smoothing length. This has important implications on the issue of particle consistency in that the discrete summation form of the integral consistency relations will only depend on the number of neighboring particles within the kernel support. While this result was previously derived from detailed SPH error analyses by Vaughan et al. [23] and Read et al. [21], we find as a further implication of our analysis that C^2 kernel consistency is difficult to achieve in actual SPH simulations due to an intrinsic diffusion, which is closely related to the inherent dispersion of the particle positions relative to the mean. This implies that in practical applications SPH has a limiting second-order convergence rate.

Numerical experiments with suitably chosen test functions in two-space dimensions validate our findings for a number of well-known SPH methods, namely the standard SPH, the CSPM method of Chen et al. [5, 4], the FPM scheme of Liu and Liu [12], the MSPH method of Zhang and Batra [26], and the recently proposed methodology of Zhu et al. [28], where no corrections are required and full consistency is restored by allowing the number of neighbors to increase and the smoothing length to decrease with increasing spatial resolution. In particular, we find that when using the root mean square error (RMSE) as a model evaluation statistics, CSPM and FPM converge to only first-order accuracy, while MSPH, which was previously thought to converge to better than third order, is actually close to second order. This result implies that both CSPM and FPM have at best C^0 consistency, while MSPH has C^1 consistency. When standard SPH is run with varied number of neighbors according to the method of Zhu et al. [28], C^0 consistency is fully restored for both the estimates of the function and its derivatives. The same is observed for the CSPM and FPM methods. The results also show that with varying number of neighbors the order of consistency is not affected by particle disorder in contrast to the case where the number of neighbors is kept fixed. Although the method of Zhu et al. [28] restores only C^0 consistency for the spatial resolutions that are attainable with the use of present-day

computers, it has the advantage of being insensitive to particle disorder and yielding estimates of the function and its derivatives that converge essentially at the same rate. However, in terms of the computational cost there remains the question on the feasibility of the method for practical applications, where restoring full C^0 consistency in highly resolved calculations will demand using quite a large number of neighbors compared to conventional SPH methods where typical choices of n lie in the range ~ 12–27 in two-space dimensions and ~ 33–64 in three-space dimensions.

The results of the present analysis not only highlight the complexity of error behavior in SPH, but also show that restoring C^2 consistency, or equivalently, achieving an accuracy higher than second order, still remains a challenge.

Acknowledgement

References

References

[1] D. Avesani, M. Dumbser, A. Bellin, A new class of moving-least-squares weno-sph schemes, J. Comput. Phys. 270 (2014) 278–299.

[2] J. Bonet, T.S.L. Lok, Variational and momentum preservation aspects of smooth particle hydrodynamic formulations, Comput. Methods Appl. Mech. Engrg. 180 (1999) 97–115.

[3] T. Chai, R.R. Draxler, Root mean square error (rmse) or mean absolute error (mae)? – arguments against avoiding rmse in the literature, Geosci. Model Dev. 7 (2014) 1247–1250.

[4] J.K. Chen, J.E. Beraun, C.J. Jih, Completeness of corrective smoothed particle method for linear elastodynamics, Comput. Mech. 24 (1999) 273–285.

[5] J.K. Chen, J.E. Beraun, C.J. Jih, An improvement for tensile instability in smoothed particle hydrodynamics, Comput. Mech. 23 (1999) 279–287.

[6] W. Dehnen, H. Aly, Improving convergence in smoothed particle hydrodynamics simulations without pairing instability, Mon. Not. R. Astron. Soc. 425 (2012) 1068–1082.

[7] R.A. Gingold, J.J. Monaghan, Smoothed particle hydrodynamics - theory and application to non-spherical stars, Mon. Not. R. Astron. Soc. 181 (1977) 375–389.

[8] P. Herrera, M. Massabo, R. Beckie, A meshless method to simulate solute transport in heterogeneous porous media, Adv. Water Res. 32 (2009) 413–429.

[9] P.A. Herrera, R.D. Beckie, An assessment of particle methods for approximating anisotropic dispersion, Int. J. Numer. Meth. Fluids 71 (2013) 634–651.

[10] C. Huang, J.M. Lei, M.B. Liu, X.Y. Peng, A kernel gradient free (kgf) sph method, Int. J. Numer. Meth. Fluids 78 (2015) 691–707.

[11] S.F. Li, W.K. Liu, Moving least-square reproducing kernel method. part ii: Fourier analysis, Comput. Methods Appl. Mech. Engrg. 139 (1996) 159–193.

[12] M.B. Liu, G.R. Liu, Restoring particle consistency in smoothed particle hydrodynamics, Appl. Numer. Math. 56 (2006) 19–36.

[13] M.B. Liu, G.R. Liu, K.Y. Lam, Constructing smoothing functions in smoothed particle hydrodynamics with applications, J. Comput. Appl. Math. 155 (2003) 263–284.

[14] W.K. Liu, S.F. Li, T. Belytschko, Moving least-square reproducing kernel method (i). methodology and convergence, Comput. Methods Appl. Mech. Engrg. 143 (1997) 113–154.

[15] L.B. Lucy, A numerical approach to the testing the fission hypothesis, Astron. J. 82 (1977) 1013–1024.

[16] F. Macià, L.M. González, J.L. Cercos-Pita, A. Souto-Iglesias, A boundary integral sph formulation, Prog. Theor. Phys. 128 (2012) 439–462.

[17] J.J. Monaghan, Smoothed particle hydrodynamics, Annu. Rev. Astron. Astrophys. 30 (1992) 543–574.

[18] J.J. Monaghan, Smoothed particle hydrodynamics, Rep. Prog. Phys. 68 (2005) 1703–1759.

[19] J.J. Monaghan, J.C. Lattanzio, A refined particle method for astrophysical problems, Astron. Astrophys. 149 (1985) 135–143.

[20] P.W. Randles, L.D. Libersky, Smoothed particle hydrodynamics: Some recent improvements and applications, Comput. Methods Appl. Mech. Engrg. 139 (1996) 375–408.

[21] J.I. Read, T. Hayfield, O. Agertz, Resolving mixing in smoothed particle hydrodynamics, Mon. Not. R. Astron. Soc. 405 (2010) 1513–1530.

[22] G.L. Vaughan, The sph equations for fluids, Int. J. Numer. Methods Engng. 79 (2009) 1392–1418.

[23] G.L. Vaughan, T.R. Healy, K.R. Bryan, A.D. Sneyd, R.M. Gorman, Completeness, conservation and error in sph for fluids, Int. J. Numer. Meth. Fluids 56 (2008) 37–62.

[24] R. Vignjevic, J. Campbell, Review of development of the smooth particle hydrodynamics (sph) method, Review of development of the smooth particle hydrodynamics (SPH) method, Springer, Dordrecht, 2009, pp. 367–396.

[25] H. Wendland, Piecewise polynomial, positive definite and compactly supported radial functions of minimal degree, Adv. Comput. Math. 4 (1995) 389–396.

[26] G.M. Zhang, R.C. Batra, Modified smoothed particle hydrodynamics method and its application to transient problems, Comput. Mech. 34 (2004) 137–146.

[27] G.M. Zhang, R.C. Batra, Symmetric smoothed particle hydrodynamics (ssph) method and its application to elastic problems, Comput. Mech. 43 (2009) 321–340.

[28] Q. Zhu, L. Hernquist, Y. Li, Numerical convergence in smoothed particle hydrodynamics, Astrophys. J. 800 (2015) id. 6, 13 pp.
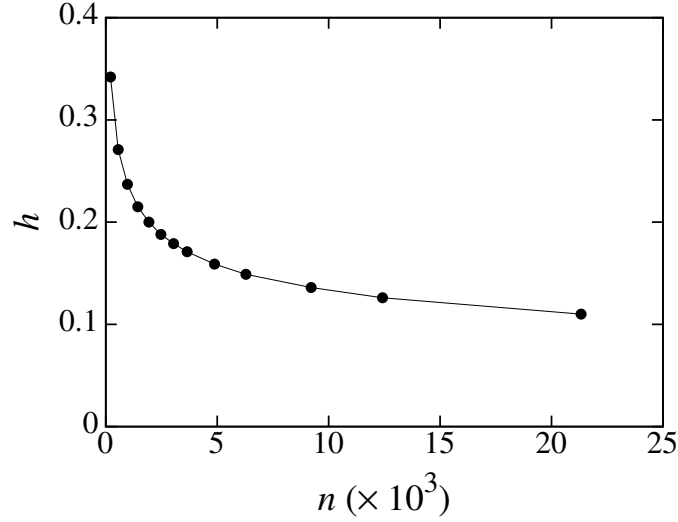
Figure 1: Dependence of the smoothing length, h, on the number of neighbors, n, as calculated using the scaling relation $h \approx 1.29 n^{-0.247}$.
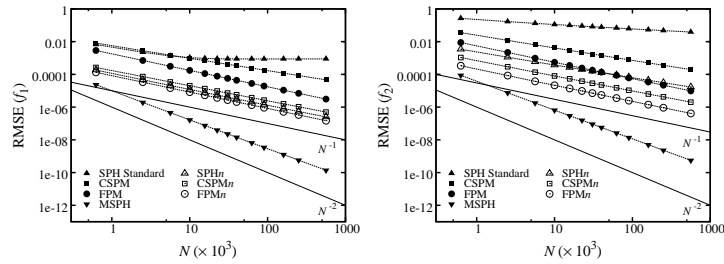

Figure 2: Convergence rates of the different SPH methods for the estimates of f_1 (left) and f_2 (right) as a function of the total number of particles, N, as obtained for a perfectly regular distribution of particles. The N^{-1} and N^{-2} trends are shown for comparison. The slopes of the straight lines for each method are given in Table 2.
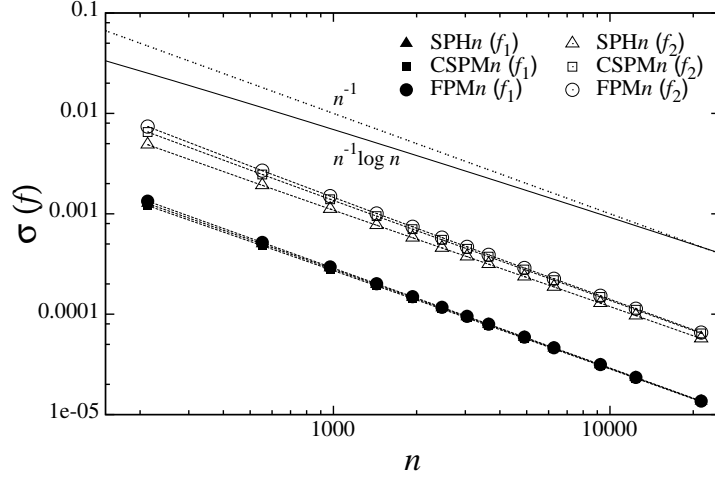
23

Figure 3: Standard deviation of the estimates of f_1 and f_2 as a function of n as obtained for a perfectly regular configuration of particles. The n^{-1} and $n^{-1} \log n$ trends are displayed for comparison. The slopes of the straight lines are: -0.962 (SPHn), -1.0 (CSPMn), -1.02 (FPMn) for the estimates of f_1 (filled markers) and -0.985 (SPHn), -0.976 (CSPMn), -0.995 (FPMn) for the estimates of f_2 (empty markers).
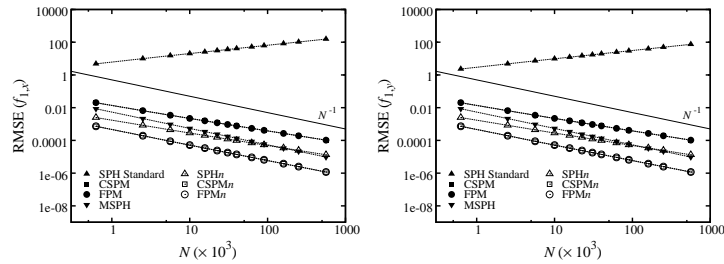
Figure 4: Convergence rates of the different SPH methods for the estimates of the first-order derivatives of f_1, $f_{1,x}$ (left) and $f_{1,y}$ (right), as a function of the total number of particles, N, for a perfectly regular distribution of particles. The N^{-1} trend is shown for comparison. The slopes of the straight lines are listed in Table 2.
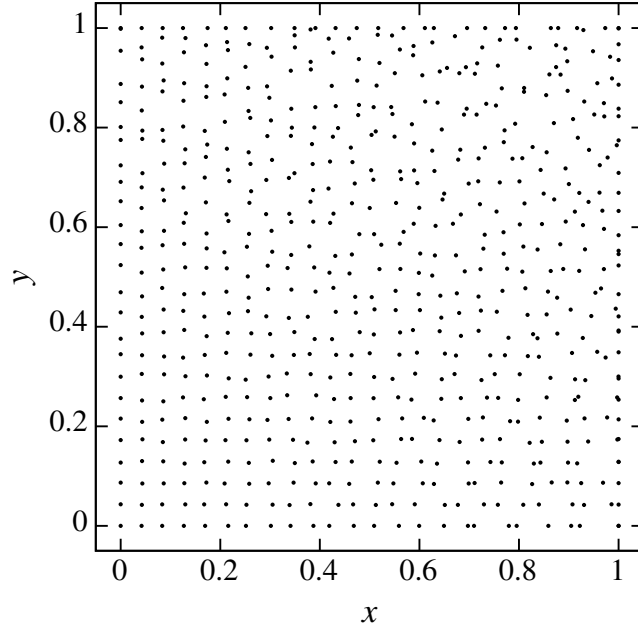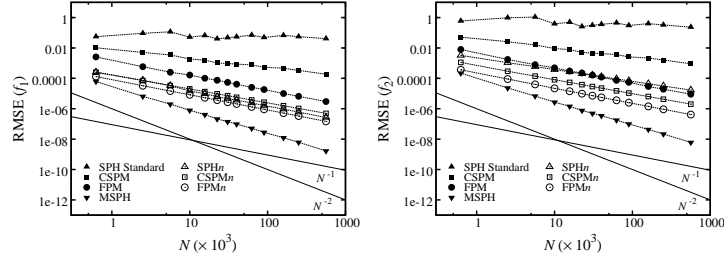
24
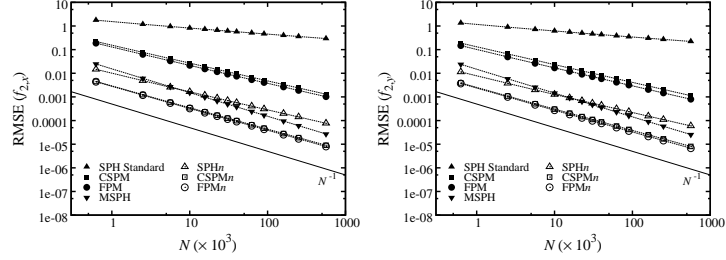
Figure 5: Convergence rates of the different SPH methods for the estimates of the first-order derivatives of f_2, $f_{2,x}$ (left) and $f_{2,y}$ (right), as a function of the total number of particles, N, for a perfectly regular distribution of particles. The N^{-1} trend is shown for comparison. The slopes of the straight lines are listed in Table 2.

Figure 6: Irregular particle distribution for the lowest resolution case ($N = 625$) in a two-dimensional domain $[0,1] \times [0,1]$. The same degree of particle disorder is maintained for all higher resolutions.

Figure 7: Convergence rates of the different SPH methods for the estimates of f_1 (left) and f_2 (right) as a function of the total number of particles, N, for an irregular distribution of particles. The N^{-1} and N^{-2} trends are shown for comparison. The slopes of the straight lines for each method are given in Table 3.
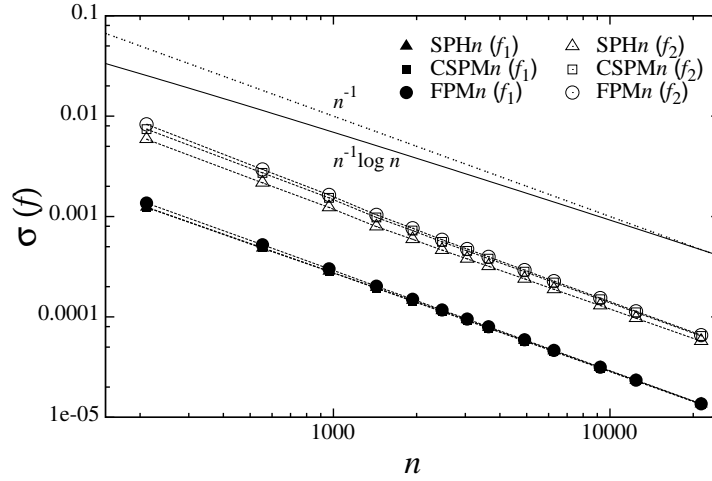

Figure 8: Standard deviation of the estimates of f_1 and f_2 as a function of n as obtained for an irregular configuration of particles. The n^{-1} and $n^{-1}\log n$ trends are displayed for comparison. The slopes of the straight lines are: -0.978 (SPHn), -0.982 (CSPMn), -0.999 (FPMn) for the estimates of f_1 (filled markers) and -1.0 (SPHn), -1.03 (CSPMn), -1.05 (FPMn) for the estimates of f_2 (empty markers).
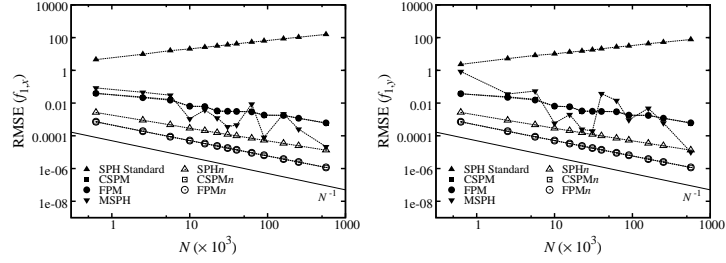
Figure 9: Convergence rates of the different SPH methods for the estimates of the first-order derivatives of f_1, $f_{1,x}$ (left) and $f_{1,y}$ (right), as a function of the total number of particles, N, for an irregular distribution of particles. The N^{-1} trend is shown for comparison. The slopes of the straight lines are given in Table 3.
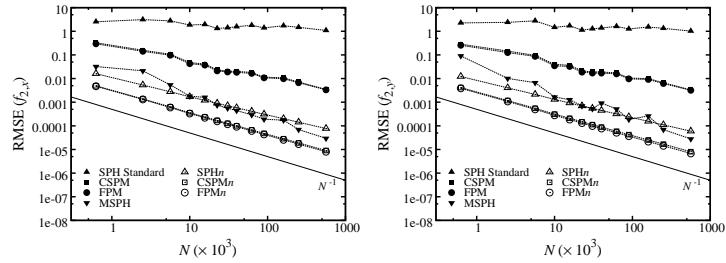

Figure 10: Convergence rates of the different SPH methods for the estimates of the first-order derivatives of f_2, $f_{2,x}$ (left) and $f_{2,y}$ (right), as a function of the total number of particles, N, for an irregular distribution of particles. The N^{-1} trend is shown for comparison. The slopes of the straight lines are given in Table 3.

27